

The rapid decline of the prompt emission in Gamma-Ray Bursts

Shlomo Dado¹, Arnon Dar¹ and A. De Rújula²

ABSTRACT

Many gamma ray bursts (GRBs) have been observed with the Burst-Alert and X-Ray telescopes of the Swift satellite. The successive ‘pulses’ of these GRBs end with a fast decline and a fast spectral softening, until they are overtaken by another pulse, or the last pulse’s decline is overtaken by a less rapidly-varying ‘afterglow’. The fast decline-phase has been attributed, in the currently-explored standard fireball model of GRBs, to ‘high-latitude’ synchrotron emission from a collision of two conical shells. This high latitude emission does not explain the observed spectral softening. In contrast, the temporal behaviour and the spectral evolution during the fast-decline phase agree with the predictions of the cannonball model of GRBs.

Subject headings: γ rays: burst-radiation mechanisms: non-thermal X-rays: flare

1. Introduction

Since the launch of the Swift spacecraft, precise data from its Burst Alert Telescope (BAT) and X-Ray Telescope (XRT) have been obtained on the spectral and temporal behaviour of the X-ray emission in γ -ray bursts (GRBs) and X-ray flashes (XRFs). These data have already been used to test the most-studied theories of long duration GRBs and their afterglows (AGs), the *Fireball* (FB) models (see, e.g., Piran 1999, 2000, 2005; Zhang & Mészáros 2004; Mészáros 2002, 2006, Zhang 2007; and references therein) and the *Cannonball* (CB) model [see, e.g., Dar & De Rújula 2004 (hereafter DD2004); Dado, Dar & De Rújula 2002, 2003, 2007a, 2007b (hereafter DDD2002, DDD2003, DDD2007a, DDD2007b), and references therein].

The general behaviour of the Swift X-ray light curves has been described as ‘canonical’ (Nousek et al. 2006; O’Brien et al. 2006; Zhang et al. 2007), and is illustrated in Figs. 1a,b, 2a

¹dado@phep3.technion.ac.il, arnon@physics.technion.ac.il, dar@cern.ch.
Physics Department and Space Research Institute, Technion, Haifa 32000, Israel.

²alvaro.derujula@cern.ch; Theory Unit, CERN, 1211 Geneva 23, Switzerland.
Physics Department, Boston University, USA.

for XRF 060218, GRB 060904a and GRB 061121. When measured early enough, the X-ray emission has peaks that coincide with the γ -ray peaks of the GRB. The prompt emission has a fast decline after the last detectable peak of the GRB. In most cases, the rapid decline ends within a couple of hundreds of seconds. Thereafter, it turns into a much flatter ‘plateau’, typically lasting thousands to tens of thousands of seconds. Finally, the X-ray light curve, within a time order of one day, steepens into a power-law decline which lasts until the X-ray AG becomes too dim to be detected. Often, there are also X-ray peaks during the fast-decline phase or even later, not coinciding with a detectable γ -ray activity. There is a continuous transition of X-ray light curve shapes from the ‘canonical’ ones to the ones that are well described by a single-power decay, e.g. GRB 061126, see Fig. 2b.

Neither the general trend, nor the frequently complex structure of the Swift X-ray data were correctly predicted by (or can be easily accommodated within) the standard FB models (see, e.g., Piran 1999, 2000, 2005; Zhang & Mészáros 2004, for reviews of the pre-Swift standard FB model, and Kumar et al. 2007; Burrows & Racusin 2007; Kocevski & Butler 2007; Urata et al. 2007; Zhang, Liang & Zhang 2007; Yonetoku et al. 2007; Liang et al. 2007 for recent comparisons with Swift data).

The situation in the CB model (Dado, Dar & De Rújula 2004, hereafter DDD2004) is different. The model offered a good description, based on a specific synchrotron-radiation (SR) mechanism, of the AGs of all ‘classical’ GRBs (DDD2002, DDD2003) of known redshift, and allowed one to extract the relevant parameters of the CBs of GRBs and XRFs. The consequent predictions for the ‘prompt’ γ -rays, based on an explicit inverse Compton scattering (ICS) mechanism, were simple and successful (DD2004). As shown in DDD2007a,b (and references therein) for ‘Swift-era’ data, the CB model, with no modification, correctly predicts the temporal and spectral behaviour of the prompt and AG phases.

In this paper we confront the Swift’s observations with the predictions of the FB and CB models for the spectral evolution during the fast-decline phase of the prompt emission. In the FB model this phase was interpreted (e.g., Mészáros 2006; Liang et al. 2006; O’Brien et al. 2006; Yamazaki et al. 2006) as the ‘curvature effect’ or ‘high-latitude’ emission of colliding shells (Fenimore et al. 1996; Kumar & Panaitescu 2000; Dermer 2004). Relative to photons centrally emitted on the line of sight to an on-axis observer, photons from off-axis latitudes arrive later and with smaller number density and energy. The consequent spectral behaviour is entirely different from that observed (see, e.g., Zhang et al. 2007). In the CB model the properties of the fast-declining phase are also dominantly ‘geometrical’. A GRB’s γ -ray pulses and their sister X-ray flares are made by ICS of light in a ‘glory reservoir’ bathing the circumburst material (DD2004). This light becomes, in a very specific manner, less abundant and more radially-directed with distance from the parent star. These simple

facts result in the correct description of the temporal behaviour and spectral evolution of GRBs, before, during, and after the fast-decline phase.

In the CB model it is possible in principle to fit the spectral energy flux of a GRB in a given energy band, as a function of time, and determine the parameters partaking in a complete prediction of the spectrum at any time in the fit interval. But the public Swift spectral data is limited to a ‘hardness ratio’ between the counting rates in the 1.5-10 keV and 0.3-1.5 keV bands (Evans et al. 2007). To convert these rates into a more explicit spectral information one must correct for instrumental efficiency, subtract the background and correct for X-ray absorption in the host galaxy, in the IGM, and in our Galaxy. The unabsorbed spectra as functions of time is not generally available. However, the unabsorbed spectral energy flux in the X-ray band, parametrized as $F_\nu \propto \nu^{-\beta} t^{-\alpha}$, is available in the form of the fitted time-dependent power-law spectral index, $\beta(t)$, for a set of X-ray light curves measured with Swift’s XRT (Zhang et al. 2007 and <http://swift.physics.unlv.edu/xrt.html>). Such a parametrization is not a faithful description of an exponentially cutoff power-law, a Band function, or the spectrum predicted by the CB model, similar to the Band function for typical parameters (DD2004). Moreover, to extract $\beta(t)$, the data from different time intervals was coadded, smoothing the time-dependence of the *effective* fitted photon index. This can be seen by comparing the effective indices $\Gamma(t)$ in $dN_\gamma/dE \propto E^{-\Gamma}$, reported in the cited web-page, with the hardness ratios reported in the Swift light-curve repository (Evans et al. 2007). The spectral indices β and Γ are related by $\beta = \Gamma - 1$.

We do not have all of the information needed for a decisive comparison between the spectral behaviour during the fast decline phase of the prompt emission. But the variation with time of the hardness ratio and of the effective spectral index during the fast decline phase are so spectacular and well correlated to the light curves, that an approximate analysis suffices to prove our points. We demonstrate this for the hardness ratios of five Swift GRBs with well sampled X-ray light curves during the fast decline phase and for fourteen other GRBs with an extracted effective time-dependent spectral index.

2. High-latitude emission in the fireball model

In the FB model, GRB pulses are produced by synchrotron radiation emitted by a shock-accelerated electrons, following collisions between conical shells ejected by a central engine (Rees & Mészáros 1994, see Zhang et al. 2007 for detailed discussion). Consider a spherical shell, arbitrarily thin, that expands with a Lorentz factor $\gamma \equiv 1/\sqrt{1 - (v/c)^2}$. Assume that when two shells collide at a radius R , all points emit isotropically in their rest frame an arbitrarily short pulse of radiation. Let $t = 0$ be the time of arrival of the first

photons on the line of sight to the center of the conical shell. Photons emitted from a shell’s polar angle θ arrive at $t = R(1 - \cos \theta)/c$. If the radiation has a power-law spectrum in the shell’s rest frame, $\tilde{\nu}^{-\beta}$, the spectral energy flux seen by the observer has the form (Kumar & Panaitescu 2000) $F_\nu \propto \nu^{-\beta} \delta^{2+\beta}$, where $\delta \equiv 1/\{\gamma[1 - (v/c) \cos \theta]\}$. Thus, for $\gamma \gg 1$, the high latitude emission from a shell collision obeys $F_\nu \propto \nu^{-\beta} (t + t_0)^{-(2+\beta)}$, with $t_0 = R/(2\gamma^2 c)$. Note that the spectral behaviour does not change during the temporal power-law decline. This is in contradiction with the observed rapid spectral softening.

To confront this problem Liang et al. (2006) *assumed* that the high-latitude spectral index β is time-dependent but the temporal index still satisfies $\alpha(t) = 2 + \beta(t)$. Although structured jet models (Mészáros, Rees & Wijers 1998; Zhang & Mészáros 2002; Ross, Lazzati & Rees. 2002) may yield a time-varying β , there is no reason why it should depend on an angle defined by the position of the observer. Indeed, the relation $\alpha(t) = 2 + \beta(t)$ is badly violated in canonical light curves (Zhang, Liang & Zhang 2007). We conclude that the curvature effect in the currently explored fireball models does not agree with the data.

3. The CB model and its predictions

In the CB model (e.g., DD2004 and references therein), GRBs and their AGs are produced by jets of highly relativistic CBs of ordinary matter (Shaviv & Dar 1995; Dar 1998; Dar & Plaga 1999). Long-duration GRBs originate from CBs ejected in core collapse supernova explosions. The ‘engine’ of short GRBs is much less well established, it could be the merger of compact objects, e.g. neutron stars, and/or mass-accretion episodes on compact objects in close binaries (e.g., microquasars), or even phase transitions of increasingly compactifying stars (neutron stars, hyper stars, or quark stars).

The pre-GRB ejecta of the parent stars create ‘windy’ environments of ‘circumburst’ material. The early luminosity of the event (a core-collapse supernova for long GRBs) permeates this semitransparent material with a temporary constituency of scattered, non-radially-directed photons: a *glory* of visible or UV light, with an approximately ‘thin-bremsstrahlung’ spectrum (DD2004). The γ -rays of a single pulse of a GRB are produced as a CB coasts through the glory. The electrons enclosed in the CB boost the energy of the glory’s photons, via inverse Compton scattering, to γ -ray energies. The initial fast expansion of the CBs and the radially-increasing transparency of the windy environment result in the exponential rise of a GRB pulse. As a CB proceeds, the distribution of the glory’s light becomes more radially directed, its density decreases. Consequently, the energy of the observed photons is continuously shifted to lower energies as their number plummets. These trends were observed in CGRO/BATSE data (Giblin et al. 2002; Connaughton 2002; Ryde & Svens-

son 2002, DD2004). During a GRB pulse the spectrum softens and the peak energy decays with time as a power law. This is also the behaviour of the X-ray flares of a GRB, which are either the low-energy tails of γ -ray pulses, or fainter and softer signals with the same origin (DDD2007a). Typically, the fast decline of the prompt emission in the γ -ray and X-ray bands is taken over, within few minutes of observer’s time, by the ‘afterglow’ –synchrotron emission from swept-in ISM electrons spiraling in the CB’s enclosed magnetic field.

The above effects can be explicitly analyzed (DD2004), and summarized to a good approximation in a *master formula* (DDD2007a) for the temporal shape and spectral evolution of the energy fluence of an ICS-generated γ -ray pulse (or X-ray flare):

$$F_E^i \propto E \frac{d^2 N_\gamma^i}{dt dE} \propto \Theta[t - t_i] e^{-[\Delta t_i/(t-t_i)]^m} \{1 - e^{-[\Delta t_i/(t-t_i)]^n}\} E \frac{dN_\gamma^i(E, t)}{dE}, \quad (1)$$

where ‘ i ’ denotes the i -th pulse, produced by a CB launched at (an observer’s) time t_i . In Eq. (1), the time scale is set by Δt_i , with $\gamma \delta c \Delta t_i/(1+z)$ the radius of transparency of the glory, within which its photons are approximately isotropic. In Δt_i time units, a pulse rises as $Exp[-1/t^m]$, $m \sim 1$ to 2, and decreases as $1/t^n$, $n \sim 2$. Finally, $E dN_\gamma^i/dE$ is the spectral function of the glory’s photons, up-scattered by the CB’s electrons, and discussed anon.

The glory has a thin thermal-bremsstrahlung spectrum: $\epsilon dn_\gamma/d\epsilon \sim (\epsilon/\epsilon_g)^{1-\alpha_g} e^{-\epsilon/\epsilon_g}$, with a typical (pseudo)-temperature $\epsilon_g \sim 1$ eV, and index $\alpha_g \sim 1$. During the γ -ray phase of a GRB, the Lorentz factor γ of a CB stays put at its initial value, for the deceleration induced by the collisions with the ISM has not yet had a significant effect (DDD2002, DD2007). Let θ be the observer’s angle relative to the direction of motion of a CB and let the corresponding Doppler factor be $\delta = 1/\{\gamma[1 - (v/c) \cos \theta]\}$. Let θ_i be the angle of incidence of the initial photon onto the CB, in the parent star’s rest system. The energy of an observed photon, Compton scattered in the glory by an electron comoving with a CB at redshift z , is given by $E = \gamma \delta \epsilon (1 + \cos \theta_i)/(1+z)$. The predicted GRB prompt spectrum is (DD2004):

$$E \frac{dN}{dE} \sim \left(\frac{E}{T}\right)^{1-\alpha_g} e^{-E/T} + b(1 - e^{-E/T}) \left(\frac{E}{T}\right)^{-p/2}. \quad (2)$$

The first term, with $\alpha_g \sim 1$, is the result of Compton scattering by the bulk of the CB’s electrons, which are comoving with it. The second term in Eq. (2) is induced by a very small fraction of ‘knocked on’ and Fermi-accelerated electrons, whose initial spectrum (before Compton and synchrotron cooling) is $dN/dE_e \propto E_e^{-p}$, with $p \approx 2.2$. Finally, T is the effective (pseudo)-temperature of the GRB’s photons:

$$T \equiv 4 \gamma \delta \epsilon_g \langle 1 + \cos \theta_i \rangle / [3(1+z)]. \quad (3)$$

For a semi-transparent glory $\langle \cos \theta_i \rangle$ would be somewhat smaller than zero.

For $b = \mathcal{O}(1)$, the energy spectrum predicted by the CB model, Eq. (2), bears a striking resemblance to the Band function (Band et al. 1993) traditionally used to model the energy spectra of GRBs. For many Swift GRBs the spectral observations do not extend to energies much bigger than T , or the value of b in Eq. (2) is relatively small, so that the first term of the equation provides a very good approximation. This term coincides with the ‘cut-off power-law’ spectrum recently used to model GRB spectra. It yields a ‘peak-energy’ (the maximum of $E^2 dN/dE$ at the beginning of a pulse) $E_p = (2 - \alpha_g) T \approx T$ for $\alpha_g \sim 1$. At later times, the CB is sampling the glory at distances for which its light is becoming increasingly radial, $\langle 1 + \cos \theta_i \rangle \rightarrow 1/r^2 \propto 1/t^2$ in Eq. (3). The value of $E_p(t)$ consequently decreases as:

$$E_p(t) \approx E_p(t_i) \left[1 - \frac{t - t_i}{\sqrt{\Delta t_i^2 + (t - t_i)^2}} \right]. \quad (4)$$

The light-curve generated by a sum of pulses is well approximated (DDD2007a) by:

$$F_E \approx \sum_i A_i \Theta[t - t_i] e^{-[\Delta t_i/(t-t_i)]^2} \left\{ 1 - e^{-[\Delta t_i/(t-t_i)]^2} \right\} [E/E_p(t)]^{1-\alpha_g} e^{-E/E_p(t)} \quad (5)$$

until ICS is overtaken by synchrotron radiation.

In X-rays the distinction between a prompt and an afterglow period can be made precise, they correspond to the successive dominance of the two radiation mechanisms: ICS and SR. The actual form of the SR-dominated AG spectral energy flux, F_ν , we have discussed very often (DDD2007a,b and references therein). Suffice it to recall that (for cases as the ones we discuss here, whose AG can be well fit with a single dominant or average CB) the shape of the observed F_ν , corrected for absorption, is determined by $\gamma_0 \theta$, and its time scale is determined by a deceleration time, t_0 , at which F_ν achromatically ‘bends down’ towards its asymptotic behaviour, $F_\nu \propto \nu^{-\beta} t^{-\beta-1/2}$. Typically $\beta \sim 1.1$ (DDD2007b).

3.1. The hardness ratio in the CB model

For a case in which the X-ray-absorption factor $A(E)$ is known, we have given enough information to predict the hardness ratio (HR) from the X-ray energy flux in a given energy band. For the late SR-dominated phase, this is trivial. A look at an X-ray light curve, such that of Fig. 1a, tells one the time at which the fast-decline ends, meaning that SR starts to dominate. From that time onwards, the HR is that corresponding to $F_E \propto E^{-\beta}$, which would be $\text{HR} \approx 0.18$ for an unabsorbed flux with $\beta = 1.1$.

In the ICS-dominated phase, the shape of the flux determines the number of flares one ought to fit, one in Fig. 1a, for instance. If one uses Eq. (5) with $\alpha_g = 1$, each pulse is fit

with 4 parameters: t_i , Δt_i , $E_p(t_i)$, and A_i . For the rapid-decline phase, it suffices to consider the main or the latest few flares, since the last factor in Eq. (5) suppresses the relative contribution of earlier flares by the time the data sample the later ones. Once the parameters are fixed, the HR is determined by the quotient of the integrals $\int dE A(E) d^2 N_\gamma / dE dt$ in the two Swift X-ray energy bands. This rosy picture is clouded by two facts: the data for the *integrated* flux in the 0.3-10 keV interval is very insensitive to the values of $E_p(t_i)$, which the fit consequently returns with very large errors; we do not know $A(E)$.

We studied numerically the HR of a pulse given by Eq. (5), in the large interval $0 < t - t_i < 10 \Delta t_i$, for an exaggerated range of E_a in $A(E) \approx \text{Exp}[-(E_a/E)^3]$. We found that

$$\text{HR}_i(t) = B e^{-[\Delta E/E_p(t_i)] \left[1 - (t-t_i)/\sqrt{\Delta t_i^2 + (t-t_i)^2}\right]^{-1}}, \quad (6)$$

is a fair approximation, with ΔE an effective interval between the bands in the HR. More explicitly, if B and $\Delta E/E_p(t_i)$ are *fit*, the approximation is good to a few % for a typical $E_p(t_i) > 200$ keV, deteriorating to $\sim 40\%$ for an extreme and atypical $E_p(t_i) = 30$ keV. We shall consequently fit B and $\Delta E/E_p(t_i)$ in comparing theory and data for the HR.

For times at which the late-time tail of a single pulse dominates, the HR satisfies

$$\text{HR}_i(t) \rightarrow B e^{-[\Delta E/E_p(t_i)] \left[2(t-t_i)^2/\Delta t_i^2\right]} \quad (7)$$

with precision increasing with t .

4. Hardness ratios: case studies

The Burst Alert Telescope (BAT) on Swift has detected nearly 250 GRBs or XRFs whose X-ray emission was followed with its X-Ray Telescope (XRT) from ~ 70 s after trigger until it faded away. Incapable of discussing all these observations, we first study five cases, which we view as representative, and which have well-sampled X-ray fluxes and hardness ratios during the fast-decline and the ensuing AG phase. They are: the ‘clean’ single-peak XRF 060218, GRB 060904a with its 4 X-ray flares during the fast decline phase, the simpler two-flare GRB 061121, the duller GRB 061126, for which the XRT observations began late and the bright GRB 061007 with an approximate single power-law afterglow.

XRF 060218: This single-peak XRF provides one of the best testing grounds of theories, given its proximity, which resulted in very good sampling and statistics. The BAT data lasted 300s, beginning 159s after trigger, with most of the emission below 50 keV (Campana et al. 2006; Liang et al. 2006). The prompt X-ray emission lasted more than 2000s, during which the peak energy evolved from 54 keV to ≤ 5 keV at the start of the fast-decline phase.

The flux and HR data are shown in Figs. 1a,c. During the afterglow phase, the HR seems to decrease gradually from ~ 0.8 at 6.2 ks to ~ 0.25 at 72 ks. In the CB model such a trend could be produced by diminishing absorption along the line of sight to the CBs.

The HR from unabsorbed synchrotron radiation with a typical $\alpha = 1.1$ is $HR \approx 0.18$, well below the reported HR for the absorbed flux of XRF 060218 (Evans et al. 2007). Pian et al. (2008) reported that the extinction derived from the equivalent width of the Na I D absorption line in the spectrum of the associated SN2006aj is $E(B - V) = 0.13 \pm 0.02$, consistent with Galactic extinction and no extinction in the host. The H column density needed to fit the Swift X-ray prompt spectrum was $NH = 6 \times 10^{21} \text{ cm}^{-2}$ (Campana et al. 2006), implying $E(B - V) \approx 1$, considerably greater than the total extinction (in the Galaxy, the intergalactic medium and the host galaxy) derived from optical emission and absorption lines, as well as from the optical colours of the afterglow, measured by Mirabal et al. (2006). These authors stress that NH is not really NH, but a proxy for the heavier elements that dominate the X-ray photoelectric absorption, and that the relatively small extinction implies a dust-deficient medium such as the stellar wind of a Wolf-Rayet progenitor, which has enough column density to be the location of this excess photoelectric X-ray absorption and relatively dust-deficient medium. The use of this large NH deduced from the prompt emission to infer the late X-ray afterglow spectrum may have resulted in the very large $\Gamma \approx 4.4 \pm 1.0$ reported in <http://swift.physics.unlv.edu/xrt.html>.

GRB 060904a: The BAT detected a weak emission of γ rays for about a minute, with several small peaks before the main burst, also seen by the Konus-Wind and Suzaku satellites (Yonetoku et al. 2007). The XRT followed the fast decline of the main burst and saw three additional flares, as shown in Fig. 1b. A rapid spectral softening was observed during both the prompt tail phase and the decline phase of the X-ray flares, see Fig. 1d. Due to a second GRB (060904b) being detected just 1.5 hours later, Swift slewed away from GRB 060904a, so that there were no data during a couple of hours until the XRT returned to follow its fading afterglow. After correcting for absorption (Yonetoku et al. 2007), the photon spectral index during the AG phase was found to be $\Gamma = 2.1 \pm 0.1$.

GRB 061121: The γ -ray burst started with a bright precursor which lasted 10s. Then, 50s later, there was a much brighter burst of γ rays. Swift had already turned its XRT when the second γ -ray flare occurred and the X-ray emission was measured during the actual event and its subsequent rapid decline, as shown in Fig. 2a. After the rapid decline, the photon spectral index, corrected for absorption, was $\Gamma = 2.05 \pm 0.15$ (Page et al. 2007).

GRB 061126: This very long burst had four main overlapping peaks, the last peak ending ~ 25 s after trigger, but low-level emission was detected until ~ 200 s later. The RHESSI satellite also detected this burst, and also saw γ -ray emission for ~ 25 s. The XRT detected

the X-ray emission only long after the prompt emission had faded. These late data are shown in Fig. 2b. The photon spectral index after correcting for absorption (Perley et al. 2007) is $\Gamma = 2.00 \pm 0.07$, and is time-independent, suggesting that the entire XRT light curve is that of the synchrotron afterglow of GRB 061126.

GRB 061007: This long bright burst lasted 75 ± 5 s. Its lightcurve showed three large peaks, and a smaller peak starting at 75 s, rising to a maximum at 79 s and declining with a very long and fast decay. The XRT began follow-up observations 80 s after trigger. The 0.3–10 keV light curve (Fig. 3a) shows a single power-law decline with a slope of 1.6 ± 0.1 . In the CB model this is the tail of a canonical AG whose ‘plateau’ ended before the XRT began its observations. The predicted photon spectral index (DDD2007b), $\Gamma = \alpha + 0.5 = 2.10 \pm 0.10$, is consistent with the best fit spectral index, $\Gamma = 2.03 \pm 0.10$, shown in Fig. 3d.

4.1. Hardness ratios: CB-model results

In the CB-model the SR-dominated X-ray afterglow, if corrected for absorption, has a time-independent photon spectral index, $\Gamma \sim 2.1$, and a constant hardness ratio. This expectation is consistent, within observational errors, with the Swift data in all the cases we considered, with the possible exception of XRF 060218, whose complex situation regarding absorption corrections we have reviewed. The spectral behaviour is much more complex during the prompt emission.

Since XRF 060218 is a single-flare event, its light curve and the evolution of its HR, shown in Figs. 1a,c, are simple. The agreement between the model expectations and the XRT observations is satisfactory. The CB-model parameters are specified in Table 1. Multi-flare events such as GRB 060904a and, to a lesser extent, GRB 061121, require multi-parameter fits; the number of peaks we fit and their relevant parameters are also specified in Table 1. The way the HR of these bursts predictably follows the ups and downs of the flux is quite impressive, compare Fig. 1b with 1d, and Fig. 2a with 2c. For GRBs 061126 (figs. 2b,c and 3b) and 061007 (figs. 3a,c,d), the available data covers only the SR-dominated X-ray AG where, as expected, the HR ratio is constant. Note in Fig. 2b that, although the late time behaviour of the flux has the shape predicted by the CB model, the measured points lie systematically above the prediction. Such a discrepancy may result from a decreasing X-ray absorption along the line of sight to the AG source. The fluxes reported in the SWIFT XRT repository (Evans et al. 2007) assume a constant absorption during the entire measurements. In the CB model, the jet of CBs moves hundreds of parsecs during the observations, and the absorption may decrease with time as the jet approaches the halo of the host galaxy.

5. CB-model results for the effective spectral index

The spectral index, $\Gamma(t) = \beta(t) + 1$ of many GRBs, extracted from an empirical power-law parametrization, $F_\nu \propto \nu^{-\beta} t^{-\alpha}$, is reported in <http://swift.physics.unlv.edu/xrt.html>, and discussed in more detail for a selected set of bright GRBs by Zhang et al. (2007). As reported in the introduction, these results on $\Gamma(t)$ may themselves be a rough description of rapidly-varying spectra potentially having an exponential energy-dependence, as in Eq. (5). Yet, we may define an *effective* index via the logarithmic derivative of the prompt ICS spectrum. For a single pulse in Eq. (5):

$$\Gamma_{\text{eff}}(E, t - t_i) = -E \left. \frac{d \log F_E}{dE} \right|_{E=\tilde{E}} = \alpha_g + \frac{\tilde{E}}{E_p(t - t_i)}, \quad (8)$$

where \tilde{E} is an effective constant energy, t is the time after trigger, and $\alpha_g \approx 1$ is defined in Eq. (2). For the synchrotron afterglow, the CB model predicts a power-law spectrum with roughly a constant photon index Γ_{SR} , and a late-time temporal power-law decline with a power-law index (DDD2007b):

$$\alpha = \Gamma_{\text{SR}} - 1/2. \quad (9)$$

In the data analysis in <http://swift.physics.unlv.edu/xrt.html>, for lack of sufficiently large statistics, different time intervals were coadded, smoothing the time-dependence of the fitted spectral index. For an ‘effective-index’ study of the results of this data analysis, a single-pulse approximation is adequate to the description of a GRB’s $\Gamma(t)$ at the end of the prompt phase and during the fast decline. In this approximation, for a pulse starting at $t=t_i$, followed by a SR-dominated afterglow, the rough CB-model prediction is:

$$\Gamma_{\text{eff}} \sim \left[1 + \frac{\tilde{E}}{E_p(t)} \right] \Theta[t_{\text{AG}} - t] \Theta[t - t_i] + \Gamma_{\text{SR}} \Theta[t - t_{\text{AG}}], \quad (10)$$

where t_{AG} is the time at which the SR ‘afterglow’ takes over the ICS ‘prompt’ emission. The assumed rather abrupt transition from the ICS-dominated first term in Eq. (10), to the second SR-dominated term, is justified by Eqs. (4, 5). Indeed, the late decline of the ICS-dominated term is exponential in the square of the time.

In Figs. 4 to 6 we compare Eq. (10) with the results for $\Gamma(t)$ for twelve GRBs from the cited web-site for which the measurements are good. The figures show how the extracted $\Gamma(t)$ reflects the expected very abrupt transition. Our simple description of the observations in terms of three parameters [t_i , $\tilde{E}/E_p(t_i)$ and Δt , listed in Table 2], is satisfactory. Also listed in Table 2 are the values of Γ_{SR} , and the values of $\alpha+1/2$ from our CB-model fits to the synchrotron-radiation afterglow. They are in fair agreement with Eq. (9).

6. Approximate results on more GRBs

Other authors have analyzed many more GRBs than we have in this paper. Zhang et al. (2007), for instance, confronting the failure of the high-latitude emission of the FB model to explain the rapid softening of the tail of the prompt emission in sixteen ‘clean-tail’ bright GRBs, proposed an empirical parametrization of the X-ray light curve during this phase. Its spectral evolution can be rewritten as a time-dependent exponentially cutoff power-law:

$$F_E \propto \left[\frac{E}{E_c(t)} \right]^{1-\alpha_g} e^{-E/E_c(t)}, \quad E_c(t) = E_c(t_i) \left(\frac{t-t_i}{t_i} \right)^{-k}. \quad (11)$$

For $t \gg t_i$, this is the evolution predicted by the CB model (DD2004), provided one identifies $E_c(t) = E_p(t)$. Indeed, $E_p(t) \approx E_p(t_i)$ for $t - t_i \ll \Delta t_i$, while for $t - t_i \gg \Delta t_i$, $E_p(t) \approx E_p(t_i) [(t - t_i)/\Delta t_i]^{-k}/2$, with $k = 2$, see Eqs. (4,7). These limiting behaviours may be interpolated by the empirical parametrization of Zhang et al. (2007), in their chosen narrow range of t , with a constant $k \leq 2$ (they find $1 \leq k \leq 1.6$). These authors also discern GRBs without a rapid spectral softening during the fast decline. These seem to us to be cases whose spectral evolution is poorly measured, or cases, like GRBs 061126 and 061007, whose ‘fast decline phase’ is not the end of the prompt emission but the late decline of a canonical AG whose plateau phase ended before the beginning of the XRT observations (DD20007b).

7. Conclusions

The spectrum of the γ -ray peaks and X-ray flares of a GRB or an XRF is predicted in the CB model: it is the spectrum of the ‘glory’s light’, Compton-boosted by the electrons in a CB (DD2004). The time evolution of the spectrum traces the voyage of the CB through this ‘target’ light. Though the model predicts the spectrum and its evolution at all frequencies and times, we have focused on the very rapid decline of the flux at the end of a pulse, and the equally swift spectral softening. Their understanding is simple: the glory’s ‘target’ light is light scattered by the circum-burst matter, and its spectrum is exponentially cutoff. Its number density, and the flux of a pulse, decrease roughly as $1/r^2 \propto 1/t^2$. Simultaneously, the target light is becoming more radial, so that the characteristic energy of the up-scattered radiation also decreases as $1/t^2$. These simple facts, explicitly reflected in the predicted ‘master formula’, Eqs. (4,5), result in an excellent description of the observations.

Lacking access to detailed spectral analyses, we have used Swift data on hardness ratios, uncorrected for X-ray absorption (Evans et al. 2007), as well as the effective spectral index of the unabsorbed spectrum reported in <http://swift.physics.unlv.edu/xrt.html>. We have demonstrated that the spectral time dependences snugly trace their expected corre-

lation to the corresponding flux variations. This test of the CB model validates it once again. Yet, carefully time-resolved absorption corrections would allow even more conclusive tests. Time-resolved corrections are important because, in the CB model, the line of sight to the hyperluminal CBs changes significantly during the long afterglow phase (e.g., DD2004) sweeping different regions of the host galaxy and the IGM. The changing absorption may induce flickering of the observed X-ray light curve and X-ray spectrum. In fact, the scintillation-like behaviour in many X-ray light curves and spectra (see Figs. 1,2,3), if not instrumental, may be due to the motion of the CBs in the host galaxy. This motion may also explain (Dado, Dar & De Rújula, in preparation) the reported time-dependence of the equivalent widths of intergalactic absorption systems detected in the afterglow of GRB 060206 (Hao et al. 2007, but see also Thone et al. 2007).

At least for GRBs or XRFs with a ‘canonical’ light curve, the transition in time from a rapidly falling X-ray decline to a much less steep plateau –accompanied by the simultaneous and even more pronounced change in the spectrum that we have studied– reflect one of the most discontinuous transitions seen in astrophysical data. In the CB model this transition is not attributed to the continued activity of a steadily energizing engine, but to the passage from one to another dominant radiation mechanism: inverse Compton scattering versus synchrotron radiation. The transition is so fast because the late decline of the ICS contribution of Eqs. (4, 5) is exponential in time, a consequence of the exponential cutoff (in energy) of the thin-bremsstrahlung spectrum of the up-scattered light (DD2004).

Acknowledgment: The authors would like to thank an anonymous referee for useful information, comments and suggestions.

REFERENCES

- Band, et al. 1993, ApJ, 413, 281
Burrows, D. N. & Racusin, J. 2007, arXiv:astro-ph/0702633
Campana, S., et al. 2006, Nature, 442, 1008
Connaughton, V. 2002, ApJ, 567, 1028
Dado, S., Dar, A. & De Rújula, A. 2002, A&A, 388, 1079
Dado, S., Dar, A. & De Rújula, A. 2003, A&A, 401, 243
Dado, S., Dar, A. & De Rújula, A. 2004, A&A, 422, 381

- Dado, S., Dar, A. & De Rújula, A. 2007a, arXiv:0706.0880
- Dado, S., Dar, A. & De Rújula, A. 2007b, arXiv:0712.1527
- Dai, X., et al., 2007, ApJ, 658, 509
- Dar, A. 1998, ApJ, 500, 93
- Dar, A. & Plaga, R. 1999, A&A, 349, 259
- Dar, A. & De Rújula, A. 2004, Physics Reports, 405, 203
- Dermer, C. D., 2004, ApJ, 614, 284
- Evans, P. A. et al. 2007, A&A, 469, 379
- Fenimore, E. E., Madras, C. D., & Nayakshin, S., 1996, ApJ, 473, 998
- Giblin, T. W. et al. 2002, ApJ, 570, 573
- Hao, H., et al. 2007, ApJ, 659, 99
- Kocevski, D. & Butler, N. 2007, arXiv:0707.4478
- Kumar, P., et al. 2007, MNRAS, 376, L57
- Kumar, P. & Panaitescu, A. 2000, ApJ, 541, L51
- Liang, E. W., et al. 2006, ApJ, 646, 351
- Liang, E. W., et al. 2007, arXiv:0708.2942
- Mészáros, P. 2002, ARA&A, 40, 137
- Mészáros, P. 2006, Rept. Prog. Phys. 69, 2259
- Mészáros, P., Rees, M. J. & Wijers, R. A. M. J. 1998, ApJ, 499, 301
- Mirabal, N., et al. 2006, ApJ, 643, L99
- Nousek, J., et al. 2006, ApJ, 642, 389
- O’Brien, P. T., et al. 2006, ApJ, 647, 1213
- Page, K. L., et al. 2007, arXiv:0704.1609
- Panaitescu, A., et al. 2006, MNRAS, 369, 2059

- Perley, D. A., et al. 2007, arXiv:astro-ph/0703538
- Pian, E., 2006, *Nature*, 442, 1011
- Piran, T. 1999, *Physics Report*, 314, 575
- Piran, T. 2000, *Physics Report*, 333, 529
- Piran, T. 2005, *RvMP*, 76, 1143
- Ryde, F. & Svensson, R. 2002, *ApJ*, 566, 210
- Rossi, E., Lazzati, D. & Rees, M. J. 2002, *MNRAS*, 332, 945
- Shaviv, N. J. & Dar, A. 1995, *ApJ*, 447, 863
- Thone, C. C. et al. 2007, arXiv:0708.3448
- Urata, Y., et al. 2007, 2007arXiv0707.2826
- Yamazaki, R., et al. 2006, *MNRAS*, 369, 311
- Yonetoku, D., et al. 2007, arXiv:0708.3968
- Zhang, B. 2007, *ChJAA*, 7, 1
- Zhang, B. & Mészáros, P. 2002, *ApJ*, 581, 1236
- Zhang, B. & Mészáros, P. 2004, *IJMPA*, 19, 2385
- Zhang, B., et al. 2006, *ApJ*, 642, 354
- Zhang, B. B., Liang, E. W. & Zhang, B. 2007, *ApJ*, 666.1002

Table 1. CB-model afterglow parameters

Parameter	060218	060904a	061121	061126	061007
t_1 [s]	−1080	41.08	52.48	—	—
Δt_1 [s]	1977	16.02	12.44	—	—
$\Delta E/E_p(t_1)$	0.19	0.0452	0.061	—	—
t_2 [s]	—	252.8	96.88	—	—
Δt_2 [s]	—	27.75	18.80	—	—
$\Delta E/E_p(t_2)$	—	0.0177	0.0014	—	—
t_3 [s]	—	629.7	—	—	—
Δt_3 [s]	—	44.0	—	—	—
t_4 [s]	—	703.4	—	—	—
Δt_4 [s]	—	747.3	—	—	—
t_0 [s]	183	821	248	263	40
$\gamma\theta$	4.28	1.25	1.42	1.12	$\ll 1$
p	2.20	2.20	2.20	1.90	2.26

Table 2. Parameters in the description of the photon spectral index $\Gamma(t)$. The values of Γ_{SR} are from the Swift public data in <http://swift.physics.unlv.edu/xrt.html>. The values of $\alpha+1/2$ are from our CB-model fits to the synchrotron-radiation afterglow. In the model the two last columns ought to be equal, see Eq. (9).

GRB	t_i [s]	Δ [s]	$\tilde{E}/E_p(t_i)$	t_{AG} [s]	Γ_{SR}	$\alpha + 1/2$
061126	—	—	—	—	1.93 ± 0.12	1.95
061007	—	—	—	—	2.10 ± 0.20	2.13
070129	243	487	0.57	1050	2.28 ± 0.22	2.14
061222A	108	113	1.09	195	2.15 ± 0.08	2.15
061121	64	5.15	0.0035	161	1.99 ± 0.13	2.10
061110A	3.7	219	1.056	261	—	1.80
060814	109	295	0.68	360	2.20 ± 0.10	2.16
060729	131	146	1.48	300	2.10 ± 0.10	2.10
060510B	190	57	0.036	460	2.14 ± 0.15	—
060211A	0	325	0.44	371	2.03 ± 0.12	2.04
050814	12	365	0.54	361	1.91 ± 0.09	1.93
050724	0	154	0.23	320	1.88 ± 0.16	1.86
050717	0	194	0.19	195	1.85 ± 0.12	1.84
050716	31	96	0.037	496	1.97 ± 0.11	1.88

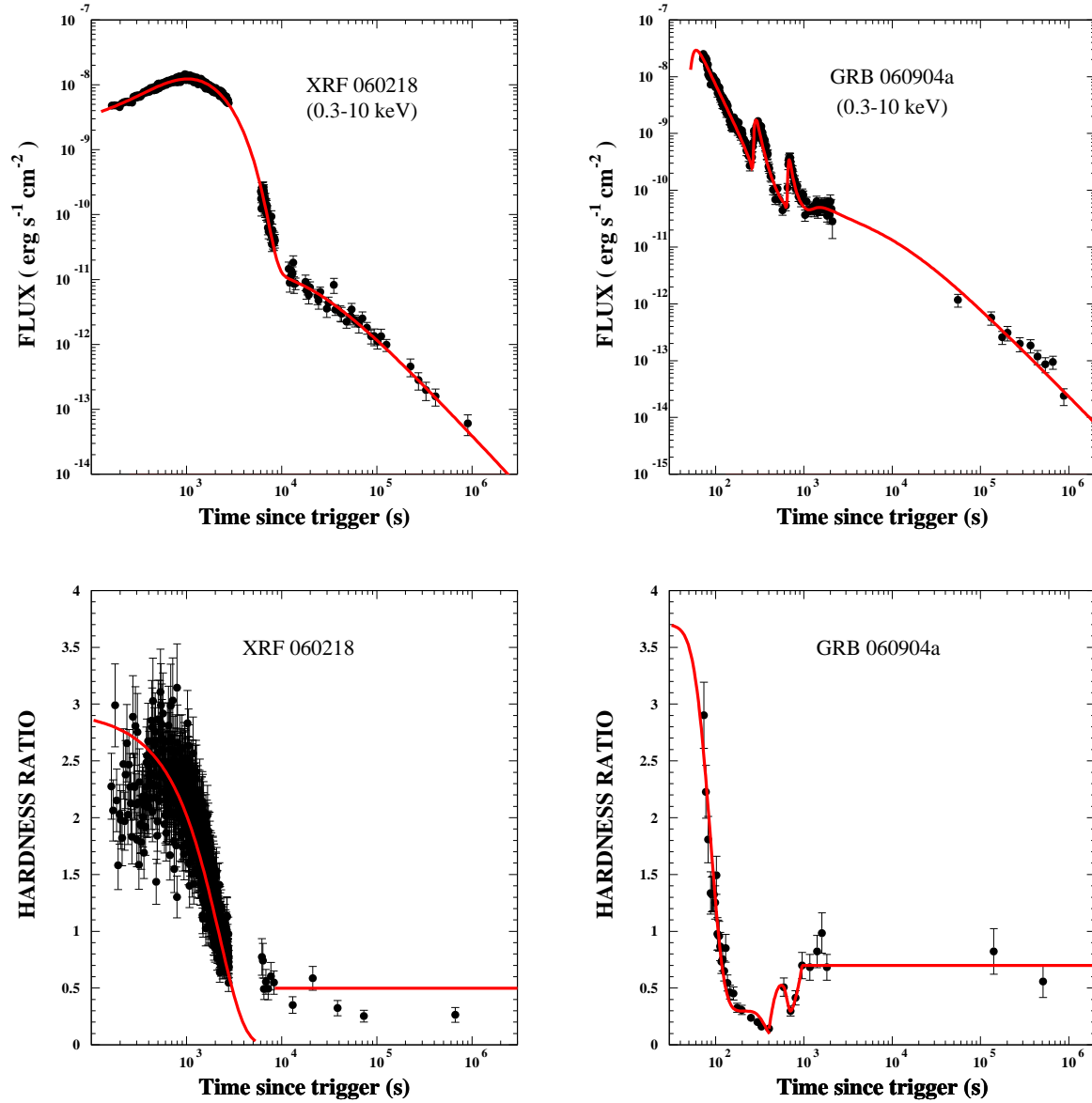


Fig. 1.— Comparisons between Swift XRT observations (Evans et al. 2007) and the CB model predictions. **Top left (a):** The light curve of XRF 060218. **Top right (b):** The light curve of GRB 060904a. **Bottom left (c):** The hardness ratio of XRF 060218. **Bottom right (d):** The hardness ratio of GRB 060904a.

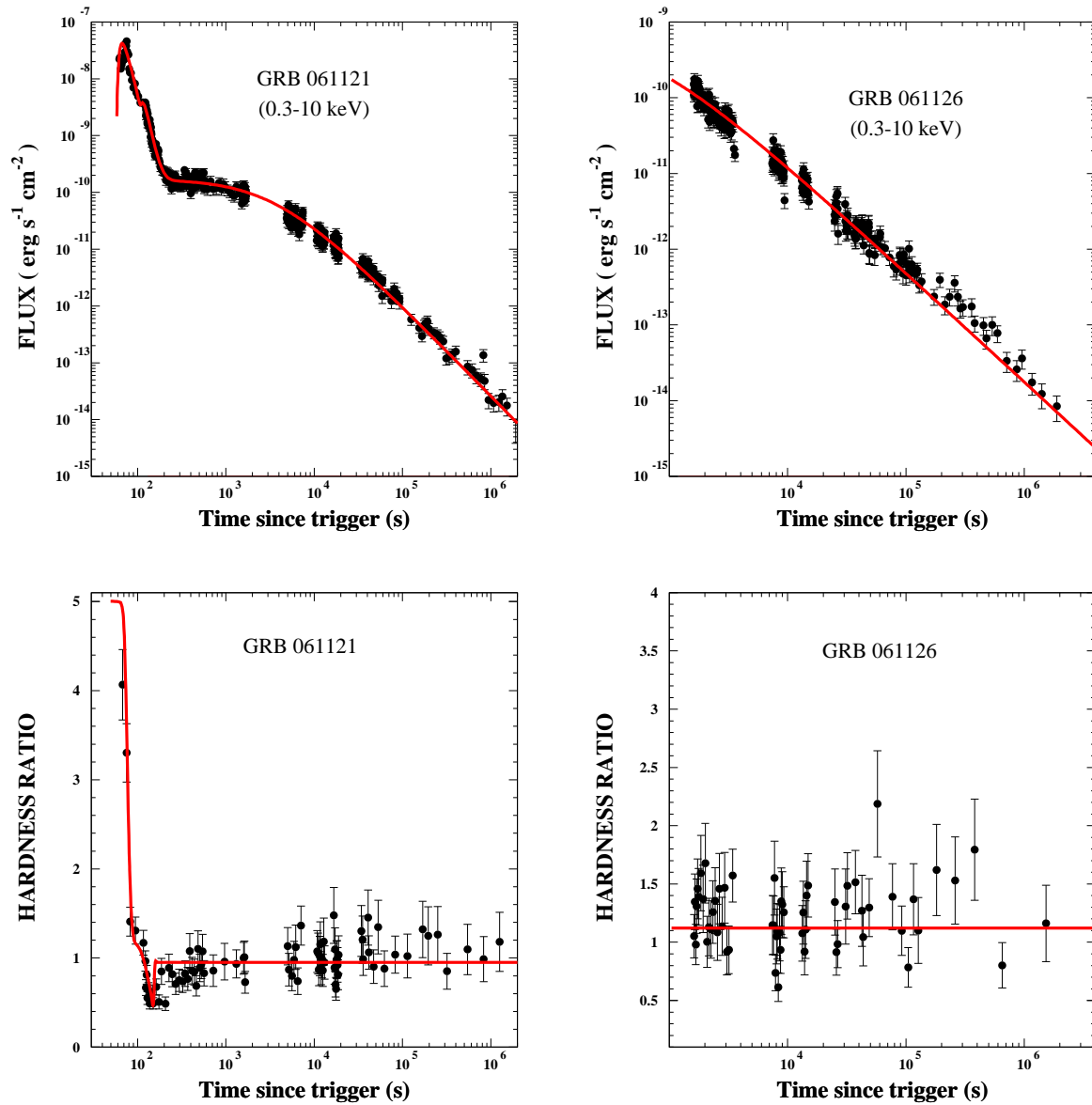


Fig. 2.— Comparisons between Swift XRT observations (Evans et al. 2007) and the CB model predictions. **Top left (a):** The light curve of GRB 061121. **Top right (b):** The light curve of GRB 061126. **Bottom left (c):** The hardness ratio of GRB 061121. **Bottom right (d):** The hardness ratio of GRB 061126.

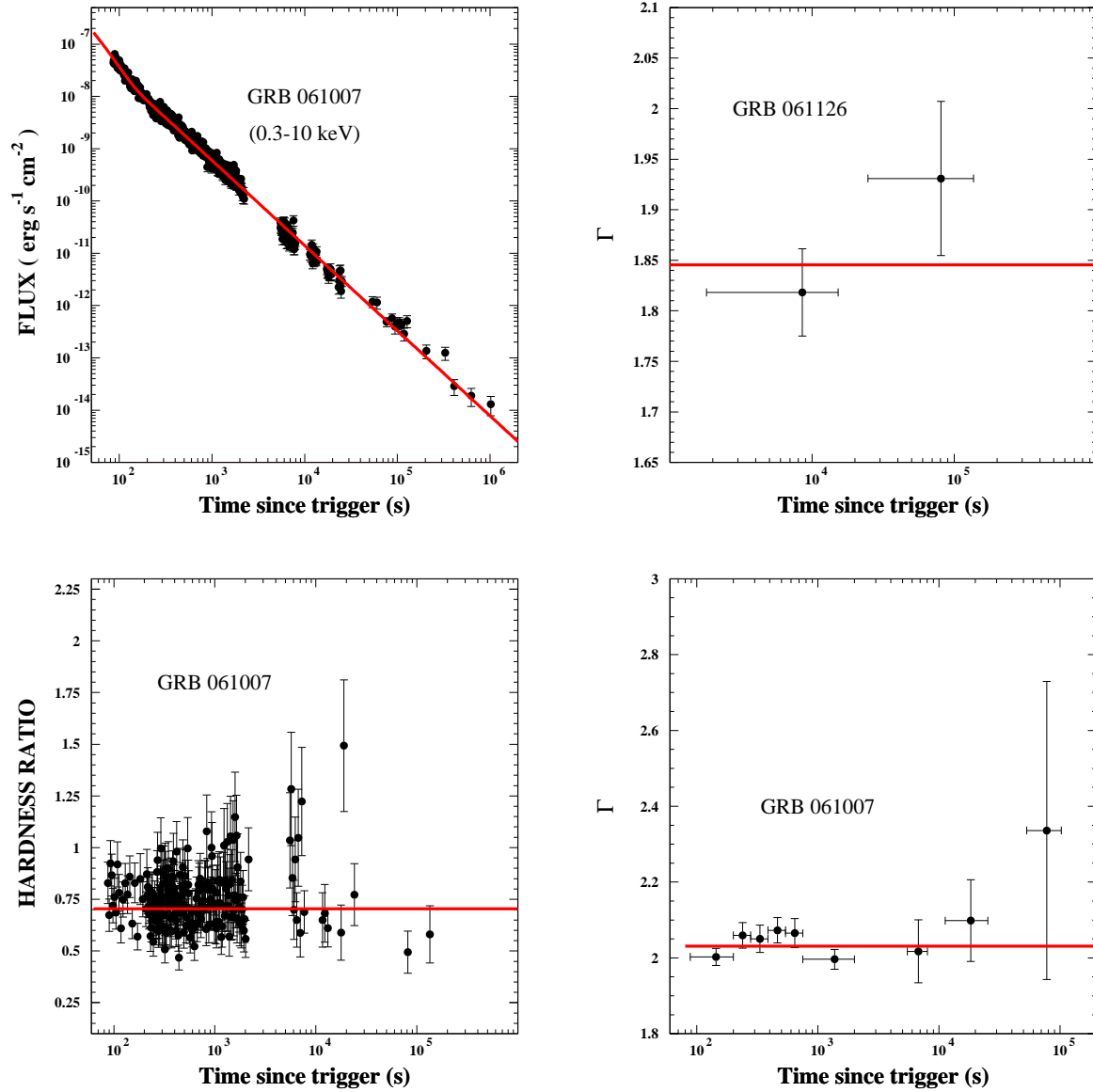


Fig. 3.— Comparisons between Swift XRT observations (Evans et al. 2007) and the CB-model predictions. **Top left (a):** The light curve of GRB 061007. **Top right (b):** The photon spectral index of GRB 061126. **Bottom left (c):** The hardness ratio of GRB 061007. **Bottom right (d):** The photon spectral index of GRB 061007. Γ values are from <http://swift.physics.unlv.edu/xrt.html>.

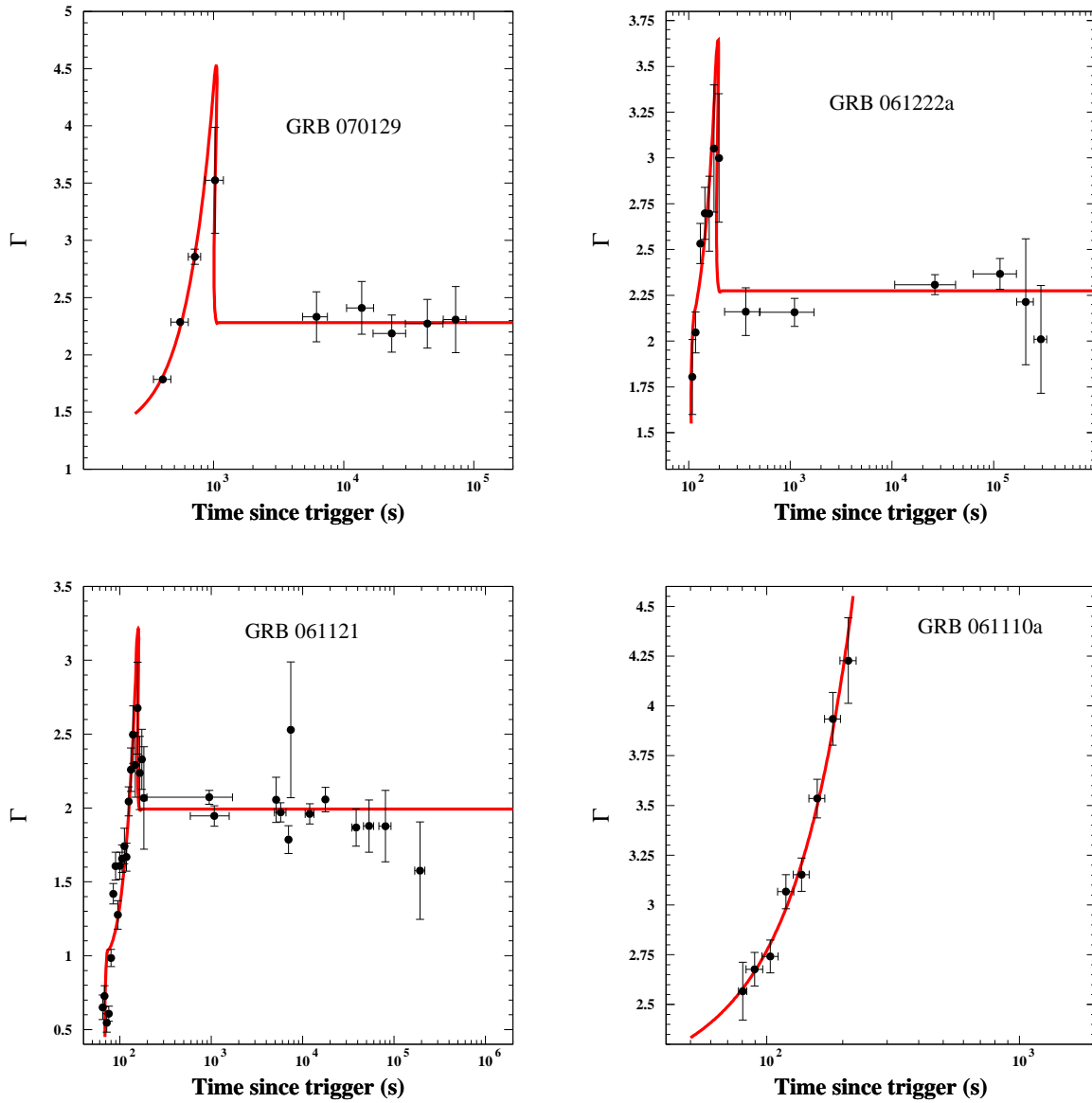


Fig. 4.— Comparisons between the effective photon spectral index in the 0.3-10 keV X-ray band as inferred from observations of GRBs with the Swift XRT, and the CB model approximate prediction, Eq. (10). **Top left (a):** GRB 070129. **Top right (b):** GRB 061222A. **Bottom left (c):** GRB 061121. **Bottom right (d):** GRB 061110A. Γ values are from <http://swift.physics.unlv.edu/xrt.html>.

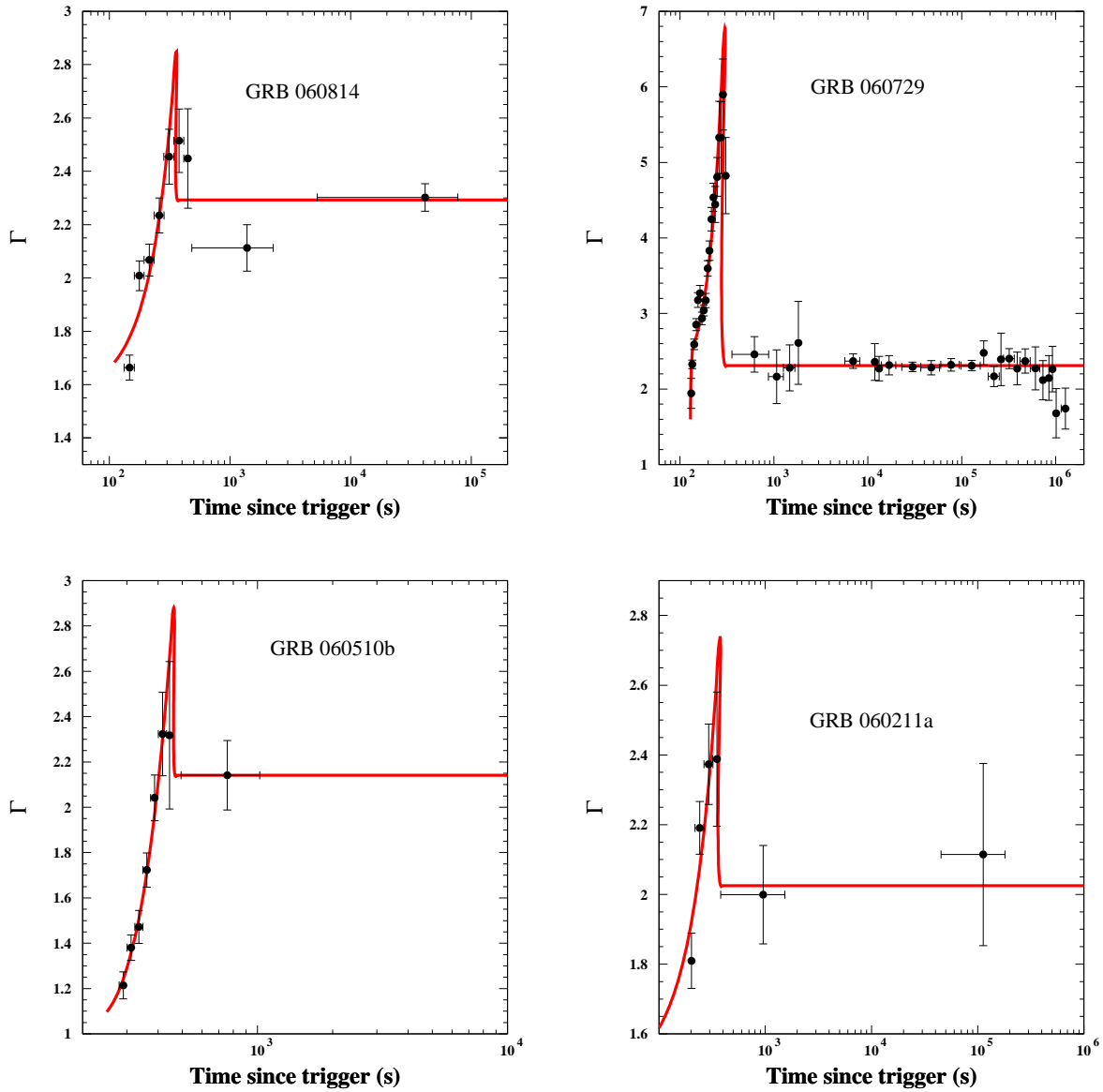


Fig. 5.— Comparisons between the effective photon spectral index in the 0.3-10 keV X-ray band as inferred from observations of GRBs with the Swift XRT, and the CB model approximate prediction, Eq. (10). **Top left (a):** GRB 060814. **Top right (b):** GRB 060729. **Bottom left (c):** GRB 060510B. **Bottom right (d):** GRB 060211A. Γ values are from <http://swift.physics.unlv.edu/xrt.html>.

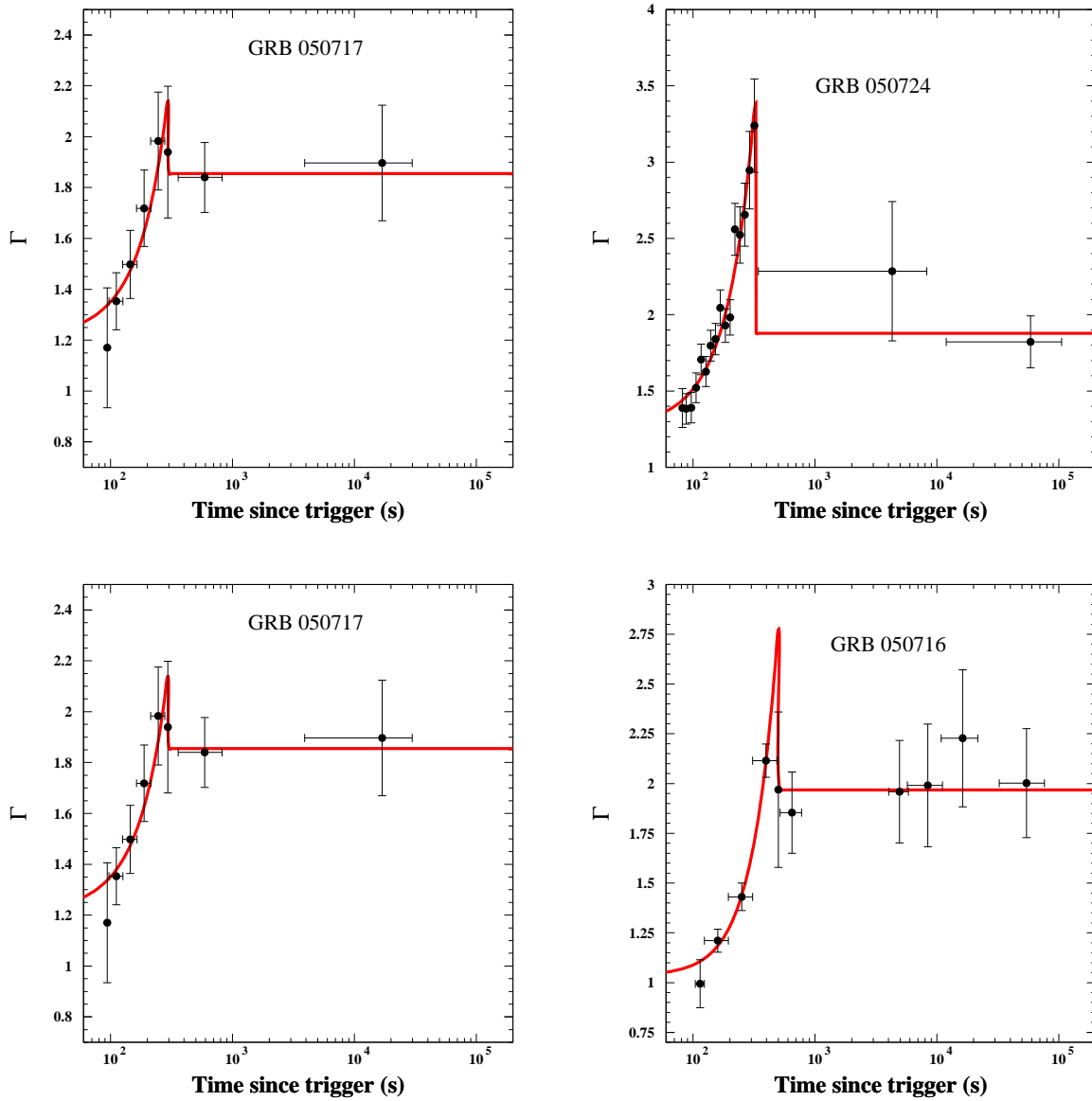


Fig. 6.— Comparisons between the effective photon spectral index in the 0.3-10 keV X-ray band as inferred from observations of GRBs with the Swift XRT, and the CB model approximate prediction, Eq. (10). **Top left (a):** GRB 050814. **Top right (b):** GRB 050724. **Bottom left (c):** GRB 050717. **Bottom right (d):** GRB 050716. Γ values are from <http://swift.physics.unlv.edu/xrt.html>.